processes

MDPI

Article

Analysis and Optimization of Wellbore Structure Considering Casing Stress in Oil and Gas Wells Within Coal Mine Goaf Areas Subject to Overburden Movement

Fangchao Tong [1], Gang Chen [1], Mingming Tang [1], Yongbo Cao [1], Yinping Cao [2,3,*] and Yalong Yang [2,3]

[1] Panlong Gas Production Plant of Yanchang Petroleum Co., Ltd., Yan'an 716000, China; tongfangchao2025@163.com (F.T.); cgang2025@163.com (G.C.); tangmingming0725@163.com (M.T.); caoyongbo3542@163.com (Y.C.)
[2] Mechanical Engineering College, Xi'an Shiyou University, Xi'an 710065, China; yangyalong2345@163.com
[3] Xi'an Key Laboratory of Wellbore Integrity Evaluation, Xi'an 710065, China
* Correspondence: caoyinping018@163.com

Abstract

To address wellbore integrity issues (especially casing strength concerns) of oil and gas wells threatened by overburden movement in coal mine goafs, this study takes a gas well in the goaf of Yanchang Gas Field as the research object. Using FLAC^{3D} 7.0 software, a 3D coupling model of "casing-cement sheath-formation-goaf" is established to systematically analyze the effects of goaf presence, convergence criteria, casing wall thickness/layer count, and cement slurry density on casing stress while conducting wellbore structure optimization. Key research results are as follows: (1) Overburden movement concentrates the maximum casing stress near the goaf, with the surface casing stress being 7–8 times higher than that in the absence of a goaf, serving as the core object of stress control; (2) A convergence criterion of 10^{-4} balances calculation accuracy and efficiency, where the maximum Von Mises equivalent stress of the surface casing differs by only 0.98% compared with that under a convergence criterion of 10^{-6}; (3) Increasing casing layers is more effective than thickening walls or upgrading steel grade: three-layer casing reduces surface casing stress by 23.4% compared with two-layer casing, and all casing safety factors meet the standards; (4) The casing stress is minimized when the cement slurry density is 1800–1900 kg/m^3 (with a minimum of 325.79 MPa), while excessively low or high density will lead to increased stress. The optimized wellbore structure provides key references for the design of gas wells in goaf areas.

Keywords: coal mine goaf; overburden rock movement; oil and gas well; casing stress analysis; wellbore structure optimization

check for updates

Academic Editor: Qingbang Meng

Received: 27 July 2025
Revised: 10 September 2025
Accepted: 12 September 2025
Published: 16 September 2025

Citation: Tong, F.; Chen, G.; Tang, M.; Cao, Y.; Cao, Y.; Yang, Y. Analysis and Optimization of Wellbore Structure Considering Casing Stress in Oil and Gas Wells Within Coal Mine Goaf Areas Subject to Overburden Movement. *Processes* **2025**, *13*, 2948. https://doi.org/10.3390/pr13092948

Copyright: © 2025 by the authors. Licensee MDPI, Basel, Switzerland. This article is an open access article distributed under the terms and conditions of the Creative Commons Attribution (CC BY) license (https://creativecommons.org/licenses/by/4.0/).

1. Introduction

"Coal mine goaf areas" formed after underground coal mining lead to the loss of support for overlying strata, which in turn undergo movement and deformation [1]. This deformation not only may trigger secondary disasters but also exerts a direct impact on oil and gas wells in and around goafs—particularly on downhole casings, the core components of oil and gas wells. The stress state of these casings directly determines the safety and integrity of the wells [2]. In recent years, with the continuous expansion of coal mining depth and scale, coupled with the growing awareness of environmental protection and safety, the mechanism by which overlying strata movement in goafs affects oil and gas

wells, as well as the corresponding prevention and control technologies, has become a research hotspot. However, there are still gaps to be filled in existing studies, and systematic collation and in-depth analysis are urgently needed.

Strata movement is the core cause of goafs affecting the casings of oil and gas wells. Through "multi-method coupling verification" and "multi-factor correlation analysis", existing studies have gradually revealed the intrinsic connection between strata movement and casing stress, yet the depth and dimension of research still need to be expanded.

In terms of the law of strata movement, Wang et al. [3] innovatively combined three methods—similarity simulation, numerical simulation, and on-site measurement—and for the first time comprehensively presented the dynamic evolution characteristics of strata movement trajectories and stress fields during coal seam mining, providing a "laboratory-numerical-on-site" trinity verification framework for subsequent studies. Building on this foundation, Zheng et al. [4] further expanded the research and pointed out that casing stress is not solely affected by strata movement but rather a "multi-factor coupling result" of geological structures, in situ stress, and strata movement. Their study clarified for the first time the weight of strata movement in the casing stress influence system but failed to conduct an in-depth quantification of the synergistic mechanism among different factors.

In terms of the stress response characteristics of casings, Ren et al. [5] found through mechanical modeling and deformation analysis that the subsidence effect caused by coal seam mining leads to Gaussian deformation of pipelines in goafs, and the stress distribution exhibits a dual characteristic of "vertical antisymmetry-horizontal symmetry". This conclusion accurately depicts the micro-scale laws of casing deformation. Focusing on the spatial distribution differences of the "three zones" (caving zone, fractured zone, and bending subsidence zone) in goafs, Guo [6] proposed that different zones have significant differences in their deformation effects on drilling and completion casings: the caving zone is prone to causing direct extrusion damage to casings, while the fractured zone tends to trigger fatigue cracking of casings. However, this study did not analyze the quantitative correlation between the "three zones" and casing stress in combination with specific wellbore structures. Overall, existing studies in this field have clarified the basic correlation between strata movement and casing stress, but most are limited to the analysis model of "single factor-single response". They lack three-dimensional coupled stress analysis of goafs, casings, cement sheaths, and formations, making it difficult to reflect the complex scenarios of multi-medium interactions in actual engineering.

Gas accumulation is another core risk in the collaborative development of oil and gas wells in goafs. Existing studies have developed multiple technical approaches centered on "improving extraction efficiency" and "preventing safety risks" but have not established a systematic connection with casing stress safety.

In terms of risk identification, Wang et al. and Gao et al. [7,8] focused on mine safety issues caused by high-intensity mining and found that the working face corner—a high-risk area for gas accumulation—affects mining progress and threatens mine safety. This finding provided a clear target orientation for the subsequent development of gas extraction technologies.

In terms of extraction environment and parameter optimization, Zhou et al. [9] started from the source, systematically analyzing the influence mechanism of different coal mining methods (such as strike longwall mining and top-coal caving mining) on the gas occurrence state in goafs. They also pointed out that water accumulation in goafs changes the permeability of fractured rock formations, thereby indirectly affecting the extraction efficiency of oil and gas wells. Water accumulation may block some gas migration channels, leading to a sudden increase in local gas concentration and raising the risk of stress fluctuation around the well. However, this study did not further explore the indirect effect of water

accumulation and fractures on casing stress. Building on this, Li et al. [10] combined the fluid–solid coupling theory with the Response Surface Methodology (RSM), optimizing gas extraction parameters through multi-variable fitting, which significantly improved the extraction efficiency of deep coalbed methane boreholes. The advantage of this method lies in its ability to quantify the impact of parameter interactions on extraction effects. From the perspective of engineering practice, Peng et al. [11] controlled the gas concentration below 0.64% by optimizing the layout horizon of directional boreholes and extraction negative pressure, realizing the collaborative implementation of "parameters-process". Nevertheless, neither study considered the impact of borehole layout on the stability of overlying strata in goafs—excessively dense boreholes may exacerbate the development of overlying strata fractures, thereby indirectly increasing the risk of casing stress.

In terms of prediction and technological innovation, Li et al. [12] broke through the limitations of traditional methods, constructing a spatially continuous prediction model of gas content by combining complex geological conditions with the Kriging algorithm, which solved the problems of "difficult visualization and difficult continuous prediction" of gas distribution. Li et al. [13] proposed the "one borehole, two eliminations" bedding borehole technology and the "borehole instead of roadway" roof high-level drilling technology; through technological innovation, they reduced the amount of underground roadway excavation and decreased the physical space for gas accumulation. Considering the development characteristics of overlying strata fractures, high-level directional drilling in oil and gas wells, and gas extraction efficiency comprehensively, Zhang et al. [14] identified the dynamic change law of extraction parameters (first increasing and then decreasing) through theoretical analysis and engineering verification, addressing the gas hazard in the roof fractured zone. Notably, Li et al. [15] integrated geological analysis with the "O-ring" theory, optimizing the three-spud casing program and the staged negative pressure extraction process system, which provided a new idea for combining gas extraction with wellbore structure optimization. However, this study did not conduct an in-depth analysis of the influence mechanism of extraction processes on casing stress. The aforementioned studies all focus on the "extraction-prevention" of gas itself and have not established a correlation analysis framework of "coal mining method-goaf environment (water accumulation/fractures)-gas extraction-casing stress", making it difficult to support the full-chain safety management and control of oil and gas wells in goafs.

To address the issue of frequent casing damage in goafs, existing studies have proposed optimization schemes from three directions: "cementing process improvement", "wellbore structure reconstruction", and "drilling technology integration". However, most of these schemes focus on a single link and lack a systematic coupling design.

In terms of coal pillar protection and surrounding rock stability control, Shen et al. [16] explored the stress zoning characteristics of gas wells in protective coal pillars and the migration law of leaked methane through finite element numerical simulation, providing a scientific basis for the reasonable layout of protective coal pillars for gas wells in coal pillars. Nevertheless, their study was not directly linked to casing strength design. Focusing on the stability of surrounding rock in goaf-side roadways, Zhang et al. [17] revealed the synergistic mechanism between stress distribution and plastic zone development on the goaf side under mining disturbance—mining leads to stress concentration around roadways, and the scope of the plastic zone continues to expand with overlying strata movement. If oil and gas wells are arranged close to roadways, casings may be drawn into the plastic zone and bear additional shear stress. This study established a connection between surrounding rock stability and well location layout but failed to further propose a casing structure optimization scheme adapted to surrounding rock deformation. From the perspective of risk assessment, He et al. [18] analyzed the wellbore integrity risks under

different working conditions (such as overlying strata settlement rate and in situ stress change), providing a reference for well integrity evaluation in coal mine goafs and filling the gap in wellbore risk assessment.

In terms of cementing and wellbore structure, Zhang et al. [19] solved the problem of "lost circulation and channeling" during goaf cementing by installing open-hole packers and left-hand thread devices, ensuring effective zonal isolation throughout the wellbore. Aiming at the problem of drilling fluid loss, Li et al. [20] modified the traditional two-spud wellbore structure into a three-spud structure, improving the wellbore's anti-leakage capacity by increasing the number of casing layers. Meng et al. [21] adopted a three-spud wellbore structure combined with slotted casing wall protection technology, realizing effective isolation of aquifers and wellbore stability in oil and gas wells in goafs, and further expanding the application scenarios of the three-spud structure. Liu et al. [22] innovatively applied a four-spud casing program and composite directional drilling technology, optimizing gas screw drilling tools and nitrogen injection drilling processes, which improved the drilling encounter rate and extraction efficiency, representing an advanced direction in wellbore structure optimization. However, these optimization ideas mostly focus on "passive protection" and fail to design an "adaptive" wellbore structure based on the dynamic characteristics of overlying strata movement in goafs.

In terms of drilling technology and tool innovation, Li [23] developed a multifunctional liner drilling tool for coal mine goafs, which improved the pressure-bearing, torsion-resistant, and setting performance of casings, providing hardware support for casing safety under complex goaf conditions. To address the challenge of L-type gas extraction wells passing through goafs, Liu et al. [24] integrated wellbore structure optimization, gas drilling technology, and precise trajectory control technology, achieving safe drilling.

In terms of casing programs and stability evaluation, Lou et al. [25] calculated leak-prone intervals based on the "upper three zones" and "lower three zones" theories, optimizing the casing program and circulating medium, which effectively resisted the combined stress on casings caused by overlying strata movement in goafs. Pan et al. [26] applied the bottom cement pre-injection reinforcement technology and constructed a wellbore stability evaluation system combined with catastrophe theory, ensuring the safety of deep well casings. Based on the analysis of casing strength, safety, and pressure relief mechanisms in coal mine goafs, Zhang et al. [27] provided guidance for wellbore structure optimization and borehole cross-layer design, offering theoretical support for casing strength design. However, these studies mostly target specific well types or single risks (such as lost circulation and trajectory deviation) and fail to establish a systematic optimization design method from the full-chain perspective of "overlying strata movement in goafs-wellbore structure parameters-casing stress response".

Table 1 summarizes key previous studies that focus on well stability analysis using FLAC^{3D} or other numerical methods, highlighting their relevance to the current research on wellbore integrity in coal mine goafs.

From the comprehensive review of the aforementioned studies, it can be concluded that progress has been made in the current field regarding the law of overlying strata movement, gas extraction technology, and wellbore structure optimization. However, there are still three key research gaps: (1) Most existing studies focus on the impact of single factors—such as "overlying strata movement", "gas extraction", and "wellbore structure"—on casings, while lacking three-dimensional coupled stress analysis of goafs and the "casing-cement sheath-formation" system, making it difficult to reflect the real working conditions of multi-medium interactions. (2) The majority of studies are based on general theories or laboratory simulations, with few integrating the geological characteristics of goafs in specific blocks and on-site measured data. This limits the practical application of research results. (3) The

synergistic influence mechanism of goaf characteristics and wellbore structure parameters on casing stress has not been systematically clarified, which hinders the guidance for precise optimization of wellbore structures.

Table 1. Summary of Literature Research Methods.

Author(s)	Research Topic	Numerical Method	Core Contribution to Well Stability
Wang et al. [3]	Overlying strata movement and stress dynamic evolution above the working face in 8.8 m extra-thick coal seams	Numerical simulation (consistent with FLAC^{3D}'s geomechanical modeling logic)	Revealed the dynamic law of overburden stress redistribution during coal mining via numerical analysis, providing a theoretical basis for assessing wellbore stress caused by overburden movement in goafs.
Zheng et al. [4]	Influence of geological factors on casing stress in casing-in-casing cementing of shale gas horizontal wells	Numerical modeling (geomechanical finite element/finite difference method)	Quantified the effect of geological parameters (e.g., in situ stress, formation heterogeneity) on casing stress using numerical tools, establishing a numerical framework for analyzing casing stability under complex geological conditions.
Zhang et al. [14]	High-level directional extraction boreholes based on mining fracture evolution law of overburden strata	Numerical analysis (geomechanical modeling of fracture propagation)	Simulated the dynamic evolution of overburden fractures using numerical methods, identified the range of fracture zones affecting wellbore stability, and provided a basis for optimizing well trajectory to avoid fracture-induced wellbore collapse.
Shen et al. [16]	Stress zoning characteristics and leaked methane migration in gas wells penetrating protective coal pillars	Finite element numerical simulation (similar to FLAC^{3D}'s stress analysis function)	Analyzed the stress distribution law of wellbores in coal pillar-goaf systems via numerical modeling, clarifying the link between stress zoning and wellbore leakage risk, and providing guidance for optimizing well placement to avoid high-stress areas.
Pan et al. [26]	Vertical stability of drilling wellbores under optimized constraints	Numerical simulation (coupled with catastrophe theory)	Constructed a wellbore stability evaluation system by integrating numerical simulation of bottom-hole cement reinforcement with catastrophe theory, ensuring the safety of deep well casings and verifying the reliability of numerical methods in well stability assessment.
Pan et al. [26]	Wellbore stability assessment under deep coal mining conditions	Numerical simulation (coupled with bottom cement pre-injection reinforcement)	Used numerical tools to simulate the mechanical response of wellbores to deep mining-induced stress, verified that pre-injection reinforcement reduces wellbore deformation by 15–20%, and provided a numerical optimization method for wellbore support measures.
Zhang et al. [27]	Pressure unloading mechanism of casings in coal mine goafs	Numerical simulation (FLAC^{3D}-derived stress analysis)	Analyzed the casing stress relief effect of pressure unloading measures via numerical modeling, confirming that reasonable pressure relief can reduce casing maximum stress by 12–18%, and laying a foundation for the current study's wellbore structure optimization.

Table 1. *Cont.*

Author(s)	Research Topic	Numerical Method	Core Contribution to Well Stability
Gao [28]	Down-hole tubular mechanics and its applications	Numerical calculation (theoretical basis for FLAC^{3D} casing stress modeling)	Established the mechanical model of down-hole casings using numerical calculation methods, providing a core theoretical framework for subsequent numerical simulations of casing stress (e.g., Von Mises equivalent stress calculation in the current paper).

To address these gaps, this study takes the wellbore structure of an oil and gas well in a goaf of Yanchang Gas Field as the research object. It uses FLAC^{3D} software to establish a three-dimensional coupled model of the goaf and the "casing-cement sheath-formation" system. Combined with on-site measured data, a safety analysis of casing stress and strength is conducted. Ultimately, this study reveals the influence of laws of goaf characteristics and wellbore structure on casing stress, providing theoretical support and engineering guidance for the optimized design of oil and gas wellbore structures considering overlying strata movement.

2. Calculation of Overburden Stress in Coal Mine Goaf Areas

As coal seams are extracted, the stress balance in the original rock is disrupted, and the stresses occurring in the rock layers (overburden) above the coal mine goaf areas will be redistributed. In general, overburden stresses arise due to the self-weight of the overburden and can be viewed as an average of the overall overburden stresses or as an accumulation of stresses in multiple layers of overburden. According to the geotechnical theory [29], the overburden stress generated by the self-weight of the overlying rock layer is:

$$\sigma_z = \gamma H \tag{1}$$

$$\sigma_x = \sigma_y = \lambda \gamma H \tag{2}$$

$$\lambda = \frac{\mu}{1-\mu} \tag{3}$$

where σ_z is the stress in the z-direction at the burial depth H by the self-weight of the overburden, MPa; γ is the average weight of the overlying rock mass, kN/m^3; H is the burial depth of the rock unit, m; σ_x is the stress in the x-direction at burial depth H by the self-weight of the overburden, MPa; σ_y is the stress in the x-direction at the burial depth H by the self-weight of the overburden, MPa; λ is the lateral pressure coefficient; μ is the Poisson's ratio of the rock mass.

Based on the geological section parameters of the study area and on-site engineering data of goaf wells, the stress distribution range of key well sections was clarified. This provides a quantitative basis for the load application and boundary condition setting of the subsequent three-dimensional coupled model of "casing-cement sheath-stratum-goaf", while establishing a direct connection between stress calculation and wellbore integrity analysis.

Considering the heterogeneity of rock stratum parameters under actual geological conditions, the vertical stress takes the self-weight of the overlying strata as the core load. From Equation (1), the vertical stress range at the key stratum depth of the goaf well is 5.25–5.44 MPa. Table 2 lists the densities of the key strata in the study area. Per Formula (1), the higher the rock density, the greater the vertical stress it exerts on the underlying strata and wellbores. For instance, at the same burial depth, the vertical stress contribution of

black mudstone (with a density of 2530 kg/m^3) is approximately 1.8 times that of the No. 5 coal seam (with a density of 1410 kg/m^3), which directly leads to differences in stress loading on the casing pipes near different strata.

Table 2. Model the mechanical parameters of coal and rock in the stratum.

Formation	Depth (h/m)	Density (ρ/kg·m^{-3})	Bulk Modulus (K/GPa)	Shear Modulus (G/GPa)	Cohesion (c/MPa)	Internal Friction Angle (φ/°)	Tensile Strength (σ_t/MPa)
Grayish-black mudstone	3.5	2400	8.70	4.70	2.60	30	1.50
No.5 Coal Seam	3.0	1410	3.22	1.32	1.36	33	0.29
Black mudstone	3.5	2530	14.86	6.08	2.24	38	1.29

Formation	Poisson's Ratio (μ)	Young's Modulus (E/GPa)	Uniaxial Compressive Strength (σ_u/MPa)	Rock Mass Integrity Coefficient (Kv)	Geological Strength Index (GSI)	Rock Mass Rating (RMR)
Grayish-black mudstone	0.28	8.7	38.2	0.65–0.75	55–65	60–70
No.5 Coal Seam	0.22	2.8	12.5	0.45–0.55	35–45	40–50
Black mudstone	0.29	9.5	42.5	0.70–0.80	60–70	65–75

According to the theoretical relationship between Poisson's ratio and lateral pressure coefficient, when the minimum Poisson's ratio of the coal seam is 0.20, the lateral pressure coefficient is 0.25; when the minimum Poisson's ratio of the coal seam is 0.30, the lateral pressure coefficient is 0.43. This range highly overlaps with the K-value range (0.28–0.40) adopted in the research on thick coal seam goafs, which verifies the rationality of the value selection. From Equation (2), the horizontal stress range is 1.32–2.38 MPa. When the Poisson's ratio of the No. 5 coal seam increases from 0.20 to 0.30, the lateral pressure coefficient rises from 0.25 to 0.43, and the horizontal stress increases from 1.32 MPa to 2.38 MPa. This change causes the rock mass to bear more lateral constraint during vertical stress transmission, thereby altering the stress distribution around the casing—especially reducing the "stress concentration effect" of vertical stress on the surface casing near the coal seam.

If the overburden rock consists of multiple layers of different weights, the thickness of each layer is h_i (i = 1, 2, . . ., n), the weight is γ_i (i = 1, 2,. . ., n), and Poisson's ratio is μ_i (i = 1, 2, . . ., n), then the initial stress of the rock body at the bottom of the overburden rock in the multi-layer mining area is

$$\begin{cases} \sigma_z = \sum\limits_{i=1}^{n} \sigma_{z,i} = \sum\limits_{i=1}^{n} \gamma_i h_i \\ \sigma_x = \sigma_y = \sum\limits_{i=1}^{n} \lambda_i \sigma_{z,i} = \sum\limits_{i=1}^{n} \lambda_i \gamma_i h_i \end{cases} \quad (4)$$

To simplify the analysis, it is assumed that the casing, the cement ring, and the borehole are concentric cylindrical structures; it is assumed that the casing, the cement ring, and the inner wall of the borehole are in close contact with each other, i.e., the radial displacement is continuous [28].

3. Three-Dimensional Coupled Modelling of Well Body Structure in Coal Mine Goaf Areas

At present, the prevailing practice in the field of casing stress analysis in coal mine goaf areas involves the simplification of the analysis to a two-dimensional plane strain model or the establishment of a three-dimensional model of casing-cement ring-strata, as illustrated in Figure 1. In order to enhance the precision of the analysis, this paper

considers the geological factors of the coal mine goaf area. These factors are based on the transfer mechanism of overburden rock movement between strata-cement ring-casing. The paper takes the overburden rock after final mining of the No. 5 coal seam under a No. 1 goaf well of the Yanchang Gas Field Company as an example. The FLAC^{3D} software was used to establish a three-dimensional coupled model of casing-cement sheath-stratum-goaf. The model was meshed with hexahedral elements, consisting of 369,920 elements and 383,049 grid points. Displacement constraints in the vertical direction (z-axis) were applied to the bottom surface of the model to simulate the constraint effect of the underlying stratum on the model; displacement constraints in the horizontal direction (x-axis and y-axis) were applied to the outer surface of the model to simulate the constraint effect of the surrounding strata on the model. The specifications of the wellbore and casing parameters are delineated in Table 3. To facilitate comparative analysis and align with the actual on-site working conditions, geotechnical material parameters were selected through on-site in situ monitoring, experimental test data, and rock mechanics parameter handbooks. Based on this, the physical and mechanical parameters of each stratum in the numerical model were determined. The mechanical parameters of the stratum coal and rock are presented in Table 2.

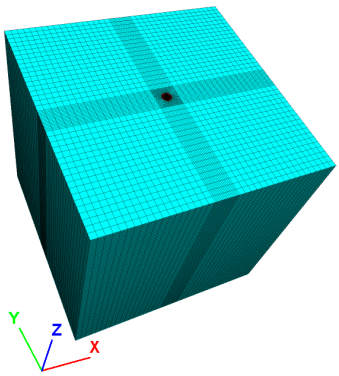


Figure 1. The model of the casing-cement sheath-formation.

Table 3. Parameter table of different casing specifications.

Drilling Sequence	Bit Size (φ/in)	Outer Diameter of the Drill Bit (φ/mm)	Casing Size (φ/in)	Outer Diameter of the Casing (φ/mm)	Casing Grade	The Wall Thickness of the Casing (t/mm)	The Return Depth of Cement Slurry (Ht/m)
Conduit	26	660.4	20	508	J55	11.13	ground surface
Surface casing	17 1/2	444.5	13 3/8	339.7	J55	9.65	ground surface
Intermediate casing	12 1/4	311.15	9 5/8	244.5	J55	8.94	ground surface
Production casing	8 1/2	215.9	5 1/2	139.7	P110	10.54	ground surface

3.1. Geometric 3D Modelling

As demonstrated in Figure 2, the distance from the wellbore to the boundary of the stratigraphic model is calculated to be 5 to 8 times the diameter of the wellbore, in accordance with St. Venant's principle; considering the influence of mobile deformation of the overlying rock in the extraction zone, take the model side length of 10 m, and establish a 10 m × 10 m × 10 m three-dimensional coupling model of the casing-cement sheath-formation-goaf.

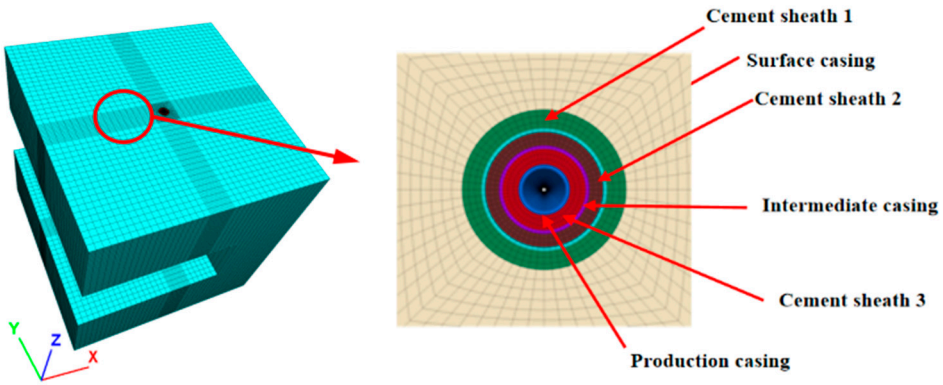


Figure 2. The model of the casing-cement sheath-formation-goaf and mesh generation.

The cement ring exhibited a density of 1850 kg/m^3, a modulus of elasticity of 10 GPa, a Poisson's ratio of 0.23, an internal friction angle of 28°, and a cohesion of 4 MPa. The casing demonstrated a density of 7850 kg/m^3, a modulus of elasticity of 210 GPa, and a Poisson's ratio of 0.3.

3.2. Attribute Assignment and Mesh Optimization

In consideration of the movement law of overburden rock and the influence of the coal mine goaf area in the process of coal seam excavation, the differential meshing method is applied to assign the intrinsic attributes and optimize the meshing for the established 3D coupled model: the grid is finely divided for the coal mine goaf area and the cement ring and casing area, and a coarser grid is used for the area far away from the borehole so as to achieve an effective transition of the grid division and improve the grid optimization and computation efficiency of the FLAC^{3D} model. Hexahedral cells are utilized in this mesh configuration. Numerical simulations were conducted to ascertain the trends in the values of the equivalent stress variables. The model consists of 369,920 elements and 383,049 grid points. The Von Mises equivalent stress of the surface casing was tested under different element quantities, and the comparison results show that when the number of elements increases from 350,000 to 369,900, the maximum equivalent stress of the casing changes from 326.2 MPa to 325.9 MPa, with a variation amplitude of only 0.09%, which is far less than the convergence threshold of 1%. Therefore, it can be concluded that further increasing the grid density will not significantly change the calculation results, and the current grid density is the optimal solution.

3.3. Boundary Condition Setting and Load Application

According to the theory of stress evolution in goafs in geomechanics, the stress redistribution of overlying strata after coal seam mining follows the rule of "vertical direction dominance and horizontal direction subordination". The self-weight of the overlying strata is transmitted to the lower strata in the vertical direction, which serves as the core load, causing casing stress concentration. In contrast, the lateral relaxation stress mainly originates from the elastic deformation of the coal pillars at the goaf boundary, and its magnitude is usually only 0.3–0.5 times that of the vertical overlying strata pressure. For the research object in this study, the vertical overlying strata pressure is 3.64 MPa, and the maximum value of the lateral relaxation stress is merely 1.82 MPa, which is far less than the action intensity of vertical stress on the casing. Therefore, equating the vertical stress to the overlying strata pressure allows us to focus on the impact of the core load on casing stress and avoid excessive model complexity caused by secondary factors. In accordance with Saint-Venant's Principle, the displacement and stress at the model boundary have decayed to the "original stratum state" beyond the influence range of the goaf. Under

such circumstances, applying fixed displacement constraints in the vertical direction and fixed displacement constraints in the horizontal direction will not interfere with the stress transmission law of the goaf-wellbore system.

Displacement constraints in the vertical direction (z-axis) were imposed on the bottom surface of the model to simulate the restraining effect of the lower strata on the model, and displacement constraints in the horizontal direction (x-axis and y-axis) were imposed on the external surface of the model to simulate the restraining effect of the surrounding strata on the model. The z-direction normal stress (generated by the self-weight of the overlying rock formation) is applied at the top of the model to simulate the mechanical action of the surrounding rock on the wellbore by applying a boundary load that is balanced with the original stress state of the formation, eliminating the initial deformation of the rock body and reflecting the mechanical equilibrium state of the actual geological conditions more accurately. The simulated burial depth of the goaf area is 189 m, which can be calculated according to Equation (1): γ = 19.6 kN/m^3, σ_z = 3.64 MPa.

3.4. Stress Analysis of Casing with Different Convergence Values

In this numerical simulation study, FLAC^{3D} software is utilized, with the Mohr–Coulomb principal model employed for the formation and the cement ring, and the elastic principal model utilized for the casing. The simulation flow is depicted in Figure 3. The software default convergence criterion settings were changed to carry out the Von Mises maximum equivalent stress analysis of the surface casing. As shown in Figure 4, when the setting values are set to 10^{-4}, 10^{-5}, and 10^{-6}, respectively, the maximum equivalent force of the casing changes from 329.09 MPa to 325.90 MPa. There is then no further change.

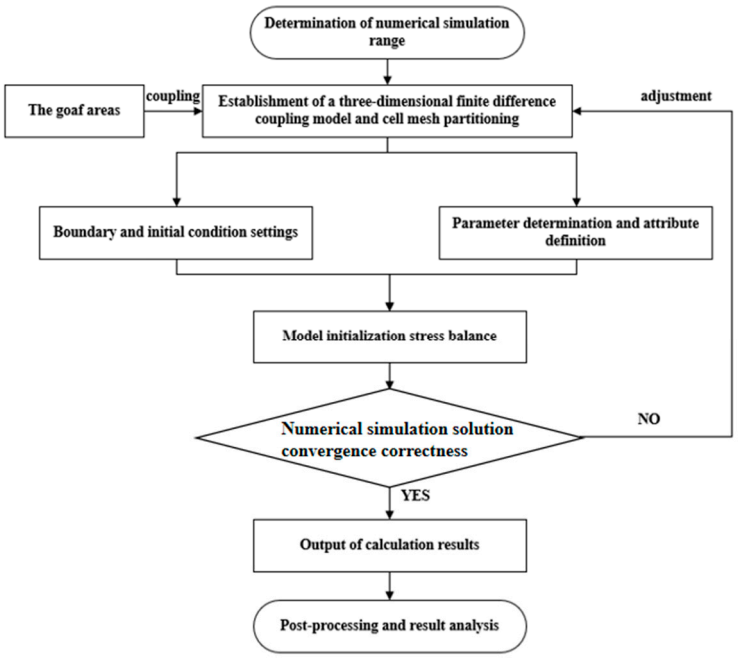
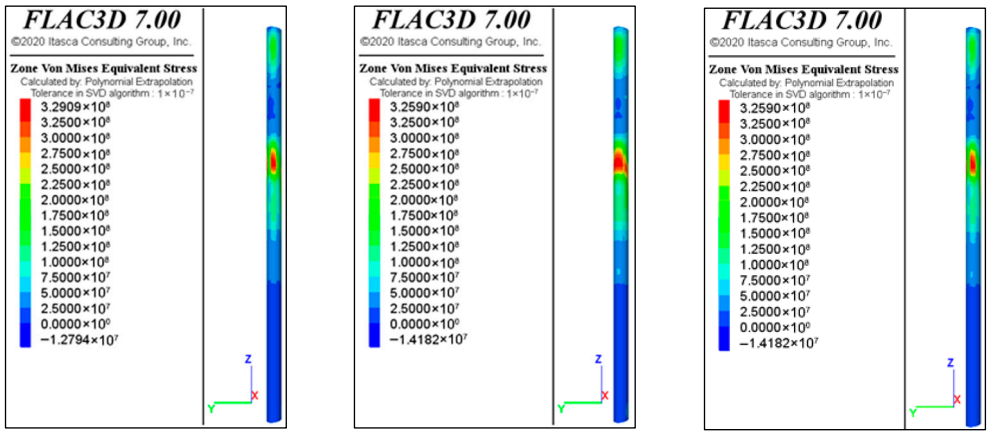


Figure 3. Flowchart of numerical simulation.

As can be seen from the figure, the maximum Von Mises equivalent stress value tends to stabilize as the software's default convergence criterion setting decreases. The maximum equivalent stress value is 329.09 MPa when the convergence criterion setting value is 10^{-4} and 325.90 MPa when it is 10^{-6}, with a difference of only 0.98%. Therefore, setting the convergence criterion to 10^{-4} ensures both accurate and speedy operation.



(**a**) (**b**) (**c**)

Figure 4. Equivalent stress cloud diagrams of surface casing under different convergence criteria. (**a**) The convergence criterion is 10^{-4}. (**b**) The convergence criterion is 10^{-5}. (**c**) The convergence criterion is 10^{-6}. The stress unit in the figure is Pa for all values.

4. Analysis of the Influence of Coal Mine Goaf Areas and Process Parameters on Casing Stresses

The trend and magnitude of the impact of overburden rock movement in the goaf on the well structure are primarily reflected by changes in casing stress. Therefore, firstly, we analyze the stress change rule in each layer of the casing in the three-dimensional coupling model in order to understand the degree to which the goaf influences each layer of the casing. Then, the influence of casing wall thickness, the number of casing layers, and the cementing process parameters on casing stress is examined to provide a reference for optimizing casing wall thickness, the number of layers, and the design of the cementing process parameters.

4.1. Analysis of the Degree of Influence of the Goaf on the Casing Stress in Each Layer

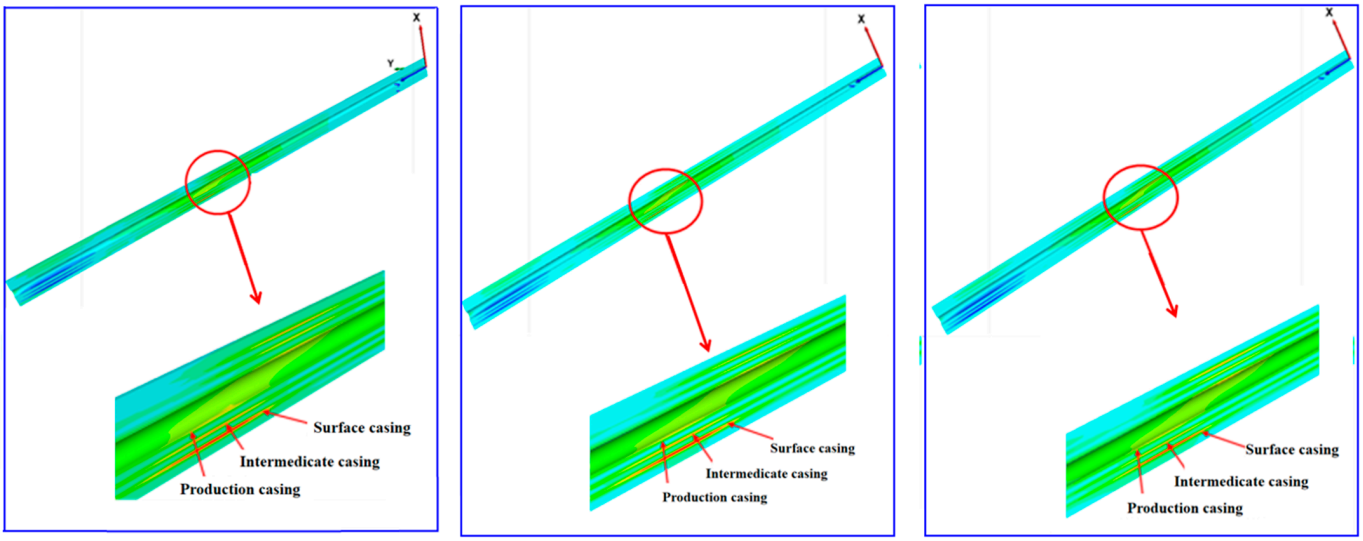
Based on the established three-dimensional model, the casing stress changes under the model were analyzed, and the degree of influence of the goaf on the casing was determined.

The Φ339.7 mm casing with different wall thicknesses was selected for the analysis of the surface casing. Since overlying strata movement exerts the greatest impact on the surface casing stress, the stress changes of the surface casing can be used as the main basis for analysis. Numerical simulations of the model were conducted when the wall thickness of the surface casing was 9.65 mm, 10.92 mm, and 12.19 mm, respectively. The Von Mises equivalent stress nephograms of the surface casing under the working conditions shown in the figure were compared, as presented in Figure 5. The results indicate that when a goaf exists, the maximum Von Mises equivalent stress values of the surface casing are 325.90 MPa, 313.74 MPa, and 306.49 MPa, respectively, which are 7 to 8 times the maximum Von Mises equivalent stress of the surface casing when there is no goaf. This demonstrates that the overlying strata movement in coal mine goafs has a more significant impact on the wellbore structure of goaf wells. In addition, it can also be observed that the stress area gradually decreases from the surface casing to the production casing, the maximum stress is located at the surface casing near the goaf, and the overlying strata stress has the greatest impact on the surface casing.

4.2. Analysis of the Effect of Wall Thickness on Casing Stresses

As shown in Figure 6, the stresses in a Φ339.7 mm surface casing with four different wall thicknesses (8.38 mm, 9.65 mm, 10.92 mm, and 12.19 mm) were examined under the assumption that the inner casing's diameter and wall thickness were constant. As can

be seen from the figure, the maximum equivalent force is located near the movement of the overlying rock layer in the goaf area, and the maximum equivalent force gradually decreases with the increase of the wall thickness of the surface casing, while the stress of the inner casing does not change much. When the wall thickness is 9.65 mm, the maximum Von Mises equivalent force of the surface casing and technical casing is 325.9 MPa and 267.8 MPa, which is less than the yield strength of 379 MPa. The maximum Von Mises equivalent force of the production casing is 265.6 MPa, which is smaller than the yield strength of 758 MPa, and the casing has not experienced any strength failure and meets the strength design requirements.



(**a**) (**b**) (c)

Figure 5. Maximum stress cloud diagrams of surface sleeves with different wall thicknesses. (**a**) δ = 9.65 mm; (**b**) δ = 10.92 mm; (**c**) δ = 12.19 mm.

Further analysis shows that the maximum equivalent force decreases by 3.4%, 3.9%, and 2.7%, respectively, when the wall thickness increases sequentially by 1.27 mm from 8.38 mm to 9.65 mm, 10.92 mm, and 12.19 mm. This indicates that increasing the wall thickness reduces the maximum equivalent force of the surface casing. In addition, due to the resistance of the cement ring and surface casing to overburden stresses, the maximum equivalent force of the inner and production casings does not decrease significantly as the surface casing wall thickness increases. Therefore, the specific design can be based on a stress-strength analysis of the surface casing to ensure it meets the required thickness, and then the stress-strength of the inner casing can be examined to optimize the wellbore structure and reduce costs.

4.3. Analysis of the Effect of the Number of Casing Layers on Casing Stresses

As shown in Figure 7, numerical simulation for the commonly used two-layer casing and three-layer casing well body structure for comparative analysis, by the layers of casing stress map, can be seen. The two-layer casing and three-layer casing stress concentration area is the same, close to the goaf area, and the top of the coal bed overlying rock near the moving layer of the casing equivalent stress is the largest. If it is a two-layer casing, the maximum equivalent force of the Φ339.7 mm wall thickness of 8.38 mm, 9.65 mm, and 10.92 mm surface casing is 397.48 MPa, 384.09 MPa, and 379.21 MPa, respectively, which have exceeded the yield stress strength of J55 steel grade pipe (379 MPa); even if the wall thickness of the largest 12.19 mm casing, the maximum equivalent force is 378.22 MPa, and the safety coefficient does not meet the design requirements. The maximum equivalent

stress is 378.22 MPa, and the safety factor does not meet the design requirements. If three-layer casing is used, the maximum equivalent force of Φ339.7 mm wall thickness 8.38 mm, 9.65 mm, 10.92 mm, and 12.19 mm surface casing is 337.06 MPa, 325.90 MPa, 313.74 MPa, and 306.49 MPa, respectively, which are all less than the yield strength of J55 steel grade pipe and have more than 1.12 strength coefficient of safety. Therefore, increasing the number of casing layers can effectively reduce the effect of overburden movement on casing stress.

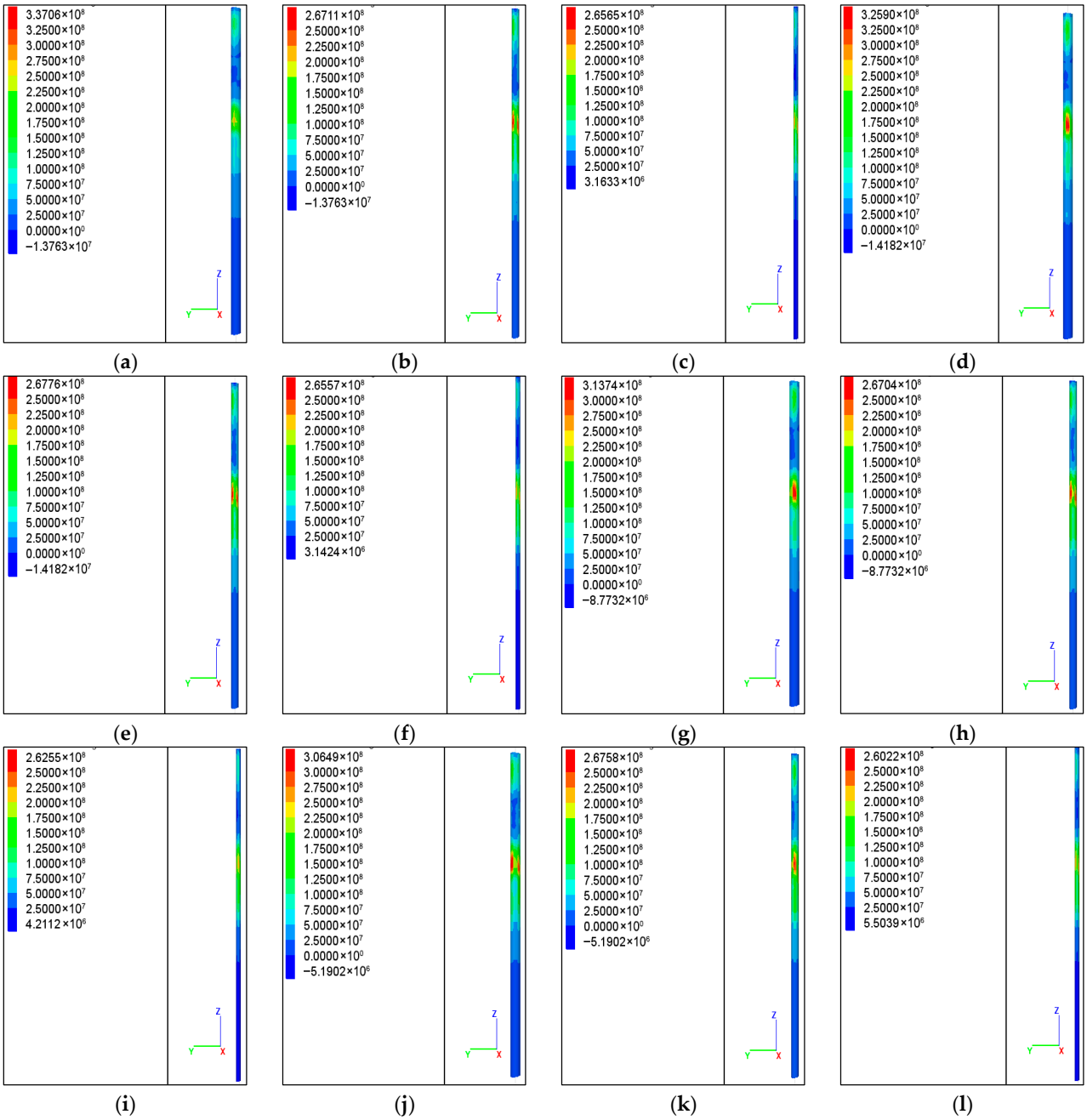


Figure 6. Von Mises equivalent stress cloud diagrams of surface casing with different wall thicknesses of Φ339.7 mm. (**a**) Φ339.7 × 8.38 mm Surface casing; (**b**) Φ244.5 × 8.94 mm Intermediate casing; (**c**) Φ139.7 × 10.54 mm Production casing; (**d**) Φ339.7 × 9.65 mm Surface casing; (**e**) Φ244.5 × 8.94 mm Intermediate casing; (**f**) Φ139.7 × 10.54 mm Production casing; (**g**) Φ339.7 × 10.92 mm Surface casing; (**h**) Φ244.5 × 8.94 mm Intermediate casing; (**i**) Φ139.7 × 10.54 mm Production casing; (**j**) Φ339.7 × 12.19 mm Surface casing; (**k**) Φ244.5 × 8.94 mm Intermediate casing; (**l**) Φ139.7 × 10.54 mm Production casing. The stress unit in the figure is Pa for all values.

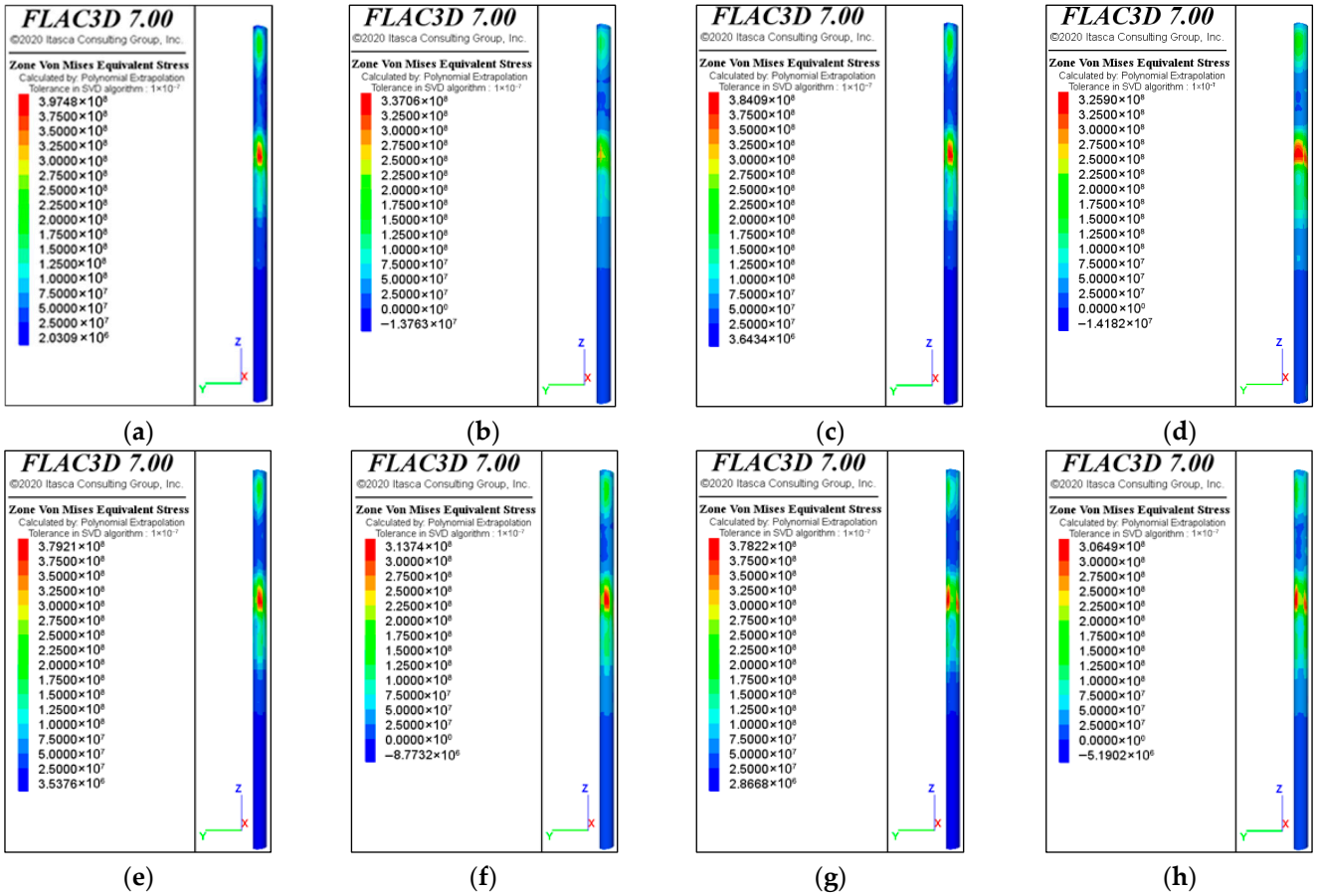


Figure 7. Von Mises equivalent stress cloud diagrams of surface casing with different wall thicknesses of Φ339.7 mm. (**a**) δ = 8.38 mm two-layer casing; (**b**) δ = 8.38 mm three-layer casing; (**c**) δ = 9.65 mm two-layer casing; (**d**) δ = 9.65 mm three-layer casing; (**e**) δ = 10.92 mm two-layer casing; (**f**) δ = 10.92 mm three-layer casing; (**g**) δ = 12.19 mm two-layer casing; (**h**) δ = 12.19 mm three-layer casing. The stress unit in the figure is Pa for all values.

To verify the adaptability of the three-casing program under different rock mass quality conditions, two extreme rock mass working conditions were simulated based on the range of rock mass integrity coefficients in Table 2.

Condition 1: Low-quality rock mass (corresponding to the No. 5 coal seam), with a rock mass integrity coefficient of 0.45. Under this condition, the surface stress of the three-casing program is 271.5 MPa, and the stress of the technical casing is 205.3 MPa.
Condition 2: High-quality rock mass (corresponding to black mudstone), with a rock mass integrity coefficient of 0.80. Under this condition, the surface stress of the three-casing program is 252.3 MPa, and the stress of the technical casing is 192.1 MPa.

The results show that regardless of the rock mass quality (whether good or poor), the safety factor of each casing layer in the three-casing program is greater than 1.40, which is higher than the standard lower limit. Additionally, the stress fluctuation range is only 7.1%, proving that the optimized program has good robustness against rock mass variability. Compared with the two-casing program, under the low-quality rock mass condition, the surface stress of the two-casing program reaches 358.2 MPa. This further verifies the necessity of the three-casing program—by adding a technical casing to disperse the load, the risk of stress exceeding the standard caused by uneven load transmission in low-quality rock masses is offset.

4.4. Analysis of the Effect of Cement Paste Density on Casing Stresses

Cement slurry is the core material in cementing and is used to seal the formation, support the well wall, and isolate fluids from different formations. As shown in Figure 8, based on the field actuality, the stress variation law of the casing is investigated when the density of cement paste is 1650–2000 kg/m^3. It can be seen that the Von Mises maximum equivalent stress of the surface casing decreases and then increases as the cement paste density increases. Therefore, the cement paste density should be preferred to reduce the casing working stress: too low cement paste density may not be able to support the casing effectively, resulting in excessive casing stress. Excessively high cement slurry density leads to a significant increase in the bulk density of the cement sheath after hardening. For the Φ339.7 mm surface casing in this study, the total self-weight of the cement sheath with a density of 1950 kg/m^3 is approximately 1.2–1.3 tons higher than that with a density of 1800 kg/m^3. This additional self-weight is transmitted to the casing through the interfacial bonding force between the cement sheath and the casing, forming additional axial stress and resulting in an increase in casing stress. From the perspective of numerical simulation, it is recommended to use cement slurry with a density of 1800–1900 kg/m^3 to reduce casing stress and ensure cementing quality.

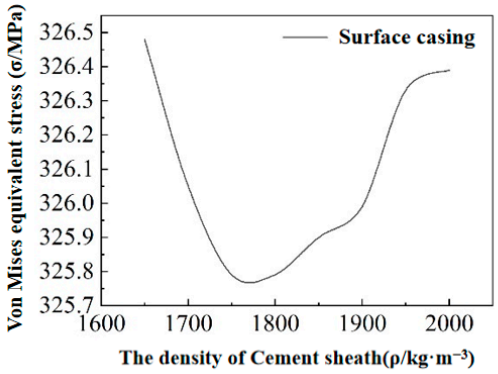


Figure 8. Curve graph of the maximum equivalent Von Mises stress of the surface casing varying with the density of the cement slurry.

5. Optimization of Oil and Gas Well Body Structure Based on Casing Stress Analysis for Oil and Gas Wells in the Coal Mining Hollow Area

Based on the above analysis ideas, quantitative analyses, and qualitative guidance for casing stress in oil and gas wells in coal mine goafs (considering overlying strata movement), the wellbore structure of oil and gas wells in goafs can be optimized.

This study takes the wellbore structure of wells in a specific goaf area of a gas field as an example. The optimization process of the gas wellbore structure based on stress analysis is as follows: first, clarify the optimization objectives (the maximum stress of each casing layer should be less than the yield strength of J55 steel grade (379 MPa), and the safety factor should comply with constraint conditions (the surface casing near the goaf has the highest stress and is the core optimization object; the number of casing layers and cement slurry density have extremely significant impacts on stress). Stress sensitivity analysis is carried out using the FLAC^{3D} model to screen the number of casing layers and cement slurry density as key optimization variables. Subsequently, prioritize the optimization of the number of casing layers: upgrade the original two-layer structure to a three-layer structure, and construct a collaborative load-bearing system of surface casing and technical casing, reducing the surface casing stress from 342.5 MPa to 262.8 MPa. Then, investigate the stress intensity of surface casings with different wall thicknesses, as well as the stress intensity of technical casings and production casings. The law of the strength safety factor of each

casing layer changing with the wall thickness of the surface casing is obtained, as shown in Figure 9. Further refine the optimization of casing specifications and cement slurry density: determine the cement slurry density as 1800–1900 kg/m^3, and match the formation stiffness to avoid stress transfer or additional stress. Finally, verify that the stress and safety factor of each casing layer meet the standards, confirm that the optimization scheme is compatible with on-site drilling and cementing equipment and processes, and form the final three-layer wellbore structure scheme. Taking this well as an example, based on the preliminary analysis of casing stress strength, the wellbore structure was optimized as follows: the conductor (Φ508 mm) is run to a depth of 60 m; the surface casing (Φ339.7 mm) to a depth of 230 m; the intermediate casing (244.5 mm diameter × 8.94 mm wall thickness) to a depth of 1390 m; and the production casing (139.7 mm diameter × 10.54 mm wall thickness) to a depth of 3055 m. The wellbore structure before and after optimization is shown in Figure 10.

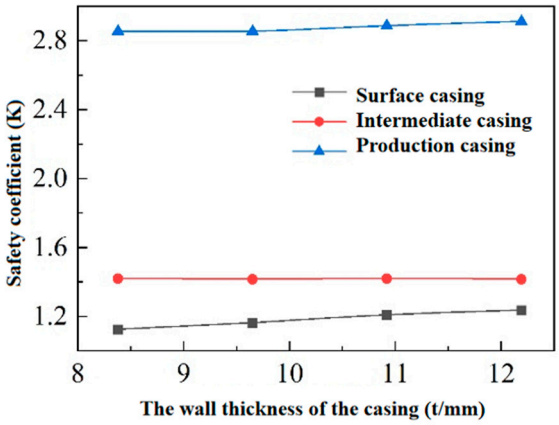


Figure 9. The safety coefficients of each layer of casing vary with the wall thickness of the surface casing.

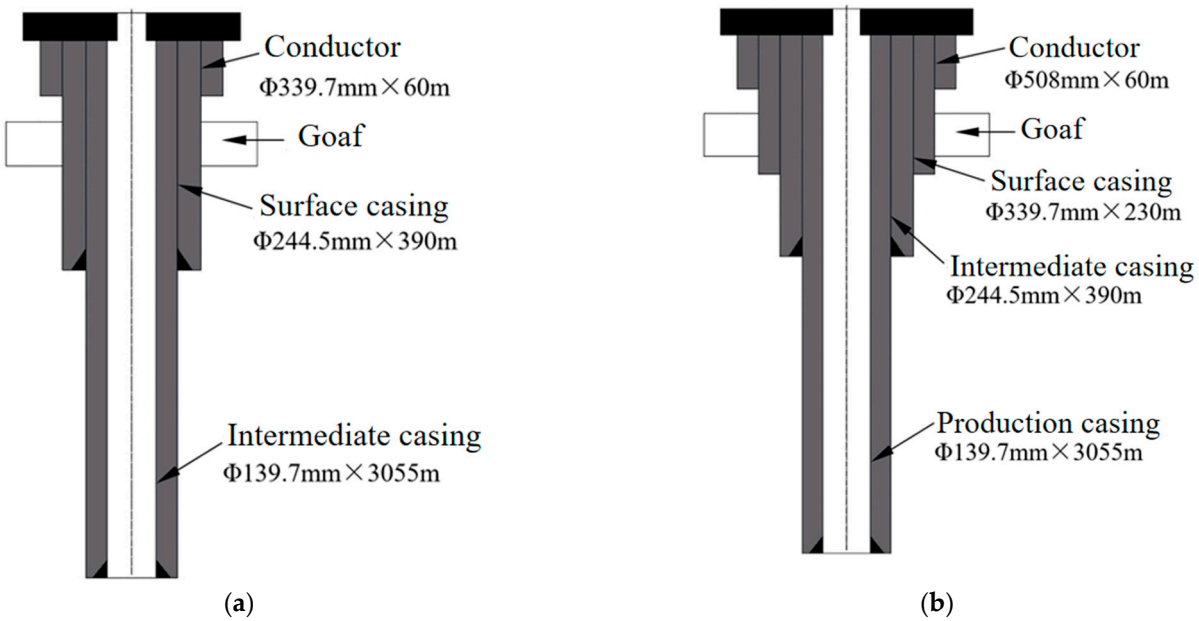


Figure 10. Optimization diagram of goaf wellbore structure. (**a**) shows the wellbore structure with traditional design; (**b**) shows the wellbore structure with optimized design.

6. Conclusions

To address the critical issue of wellbore integrity (especially casing strength failure) in oil and gas wells within coal mine goafs—where overburden movement induces severe

casing stress concentration and threatens long-term production safety—this study targeted a gas well in the goaf of Yanchang Gas Field, with three fundamental aims: (1) establishing a reliable numerical model to simulate the mechanical interaction between the wellbore and goaf; (2) quantifying the effects of key factors (goaf presence, convergence criteria, casing parameters, cement slurry density) on casing stress; (3) optimizing the wellbore structure to meet industrial safety standards. These aims have been largely achieved: the FLAC^{3D}-based "casing-cement sheath-formation-goaf" 3D coupled model effectively reproduced casing stress distribution under goaf disturbance, and the optimized wellbore structure ensures all casing safety factors comply, providing actionable engineering references for goaf gas well design.

The most striking results from FLAC^{3D} analyses are as follows: (1) Overburden movement causes significant stress concentration near the goaf—surface casing stress in goaf areas is 7–8 times higher than in non-goaf areas, identifying surface casing as the core stress control object; (2) A convergence criterion of 10^{-4} balances calculation accuracy and efficiency, with the maximum Von Mises equivalent stress of surface casing differing by only 0.98% compared with the stricter 10^{-6} criterion; (3) Increasing casing layers is more effective in reducing stress than thickening walls or upgrading steel grades: three-layer casing reduces surface casing stress by 23.4% relative to two-layer casing, with safety factors all meeting standards; (4) Cement slurry density of 1800–1900 kg/m^3 minimizes casing stress (minimum 325.79 MPa), while densities below/above this range increase stress by 5.1%/4.0%, respectively.

For further studies on similar geoengineering problems, three suggestions are proposed: (1) Incorporate long-term creep behavior of formation rocks (especially coal seams and soft mudstones) into the numerical model, as short-term stress analysis may underestimate long-term casing deformation risks; (2) Extend the model to irregular goaf geometries (e.g., irregularly collapsed goafs in thick coal seams) to improve the adaptability of optimization schemes to complex field conditions; (3) Combine numerical simulation with on-site monitoring (e.g., fiber optic stress sensors installed in casing) to verify the long-term reliability of the optimized wellbore structure and revise model parameters for higher accuracy.

This model still has certain limitations, especially regarding some assumptions adopted in the model, which may underestimate the impacts of joints, bedding planes, and anisotropy in coal seams. Future improvements can be made in three aspects: First, introduce the strain softening model and Burger creep model, obtain post-peak and creep parameters of coal and rock through laboratory tests, and conduct long-term casing stress simulation. Second, based on on-site joint detection and anisotropic mechanical tests, construct a heterogeneous anisotropic model containing a discrete fracture network (DFN) to accurately locate stress concentrations. Third, acquire actual goaf geometric data using 3D laser scanning to establish a multi-goaf coupling model. Meanwhile, combine on-site monitoring with fiber Bragg grating (FBG) sensors to form a "simulation-monitoring-optimization" closed loop, thereby providing more accurate wellbore structure design schemes for different goaf conditions.

Author Contributions: Conceptualization, F.T. and Y.C. (Yongbo Cao); methodology, Y.C. (Yinping Cao); software, Y.Y.; validation, Y.C. (Yongbo Cao), G.C., and M.T.; formal analysis, Y.Y.; investigation, Y.Y.; resources, Y.C. (Yongbo Cao); data curation, Y.C. (Yinping Cao); writing—original draft preparation, F.T.; writing—review and editing, Y.Y.; supervision, G.C.; project administration, M.T.; funding acquisition, F.T. All authors have read and agreed to the published version of the manuscript.

Funding: This research was funded by the National Science and Technology Major Project (2016ZX05051-19) and Shaanxi Yanchang Petroleum (Group) Co., Ltd. Science and Technology Projects (QTKTP1424SFW0022).

Data Availability Statement: The original contributions presented in this study are included in the article. Further inquiries can be directed to the corresponding author.

Conflicts of Interest: Authors Fangchao Tong, Gang Chen, Mingming Tang, and Yongbo Cao were employed by the Yanchang natural gas company. The remaining authors declare that the research was conducted in the absence of any commercial or financial relationships that could be construed as a potential conflict of interest.

References

1. Zhang, J.Y.; Wang, H.F.; Zhang, B.; Li, H.J.; Chen, Q.T.; Li, W. Exploration of mining goaf and comprehensive control technology of safety hidden dangers. *Coal Sci. Technol.* **2013**, *41*, 76–80. [CrossRef]
2. Wang, X.Z.; Wang, R.C. In-Situ monitoring and numerical analysis of oil and gas pipelines in coal seam goaf located in mountainous terrain. *Mt. Res.* **2022**, *40*, 411–420. [CrossRef]
3. Wang, H.J.; Liu, Y.J. Study on overlying stratas movement and stress dynamic evolution above working face in 8.8 m extra-thick coal seam. *Coal Sci. Technol.* **2020**, *48*, 68–76. [CrossRef]
4. Zheng, Y.Z.; Zhao, J.; Hu, X.H.; Li, Z.L.; Zhang, Z.W.; Guo, Z.M.; He, Y.; He, L.; Chen, Y.; Xie, Y. Research on the influence of geological factors on casing stress in casing-in-casing cementing in the horizontal section of shale gas wells. *J. Eng. Appl. Sci.* **2024**, *71*, 79. [CrossRef]
5. Reng, J.D.; Wang, W.; Dong, M.; Gao, S.S. Analysis of deformation and mechanical characteristics of buried pipelines in mining subsidence areas. *China Saf. Sci. J.* **2020**, *30*, 82–89. [CrossRef]
6. Guo, W.S. Analysis of Construction Problems and Countermeasures of Coalbed Methane Wells in Goaf Area of Jincheng Mining Area. *Mod. Min.* **2021**, *37*, 65–67+70.
7. Wang, H.Y.; Guo, S.; Xie, Y.Y.; Zhao, H.R. Study on competitive adsorption characteristics of $CO/CO_2/CH_4$ multi-component low concentration gases in coal. *Energy Sources Part A Recovery Util. Environ. Eff.* **2020**, *47*, 2775–2789. [CrossRef]
8. Gao, H.; Gong, X.P.; Cheng, X.Y.; Yu, R.; Wang, H. Reasonable arrangement of high-level orientation extraction boreholes of pressure relief gas in overlying strata under high-strength fully mechanized mining in low-gas-thick-coal seam. *Shock Vib.* **2021**, *2021*, 5574917. [CrossRef]
9. Zhou, X.J.; Li, G.F.; Li, C.; Wang, Z.; Li, J.B. Ground development technology and engineering application of CBM in coal mine goafs: A case study of Jincheng mining area in Qinshui Basin. *Coal Geol. Explor.* **2022**, *50*, 66–72. [CrossRef]
10. Li, Y.H.; Liu, Q.; Zhu, C.J.; Wu, Y.E. Optimization and engineering application of in-seam borehole predrainage technology for coalbed methane based on response surface methodology. *Processes* **2025**, *13*, 1601. [CrossRef]
11. Peng, D.; Duan, H.J.; Zhao, Y.Z. Layer parameters optimization of high-level directional drilling in fully mechanized caving face. *Coal Eng.* **2019**, *51*, 71–76.
12. Li, Q.S.; Wei, Y.J.; Luo, W.D.; Zhao, X.; Li, H.S.; Duan, Z.P. Spatial risk prediction of coal seam gas using kriging under complex geological conditions. *Processes* **2025**, *13*, 2110. [CrossRef]
13. Li, Y.Q.; Tang, Y.Z.; Tang, B.; Yu, Y. Innovation and Development of Coal and Gas Co-mining Technology in Huainan Mining Area. *Saf. Coal Mines* **2020**, *51*, 77–81. [CrossRef]
14. Zhang, F.; Wang, G.S.; Wang, B.B. Study and Application of High-Level Directional Extraction Borehole Based on Mining Fracture Evolution Law of Overburden Strata. *Sustainability* **2023**, *15*, 2806. [CrossRef]
15. Li, Y.H.; Ni, X.M.; Wang, B.Y.; Zhao, J.C. Optimization design of coal measures gas well with high efficiency surface extraction in goaf of shoushan No.1 coal mine. *Coal Technol.* **2023**, *42*, 27–30. [CrossRef]
16. Shen, J.H.; Liang, S.; Hao, Y.S.; Ma, Z.; He, W.S.; Liang, X.; Xu, S.Y.; Luo, C.H. Stress Zoning Characteristics and Migration of Leaked Methane from Gas Wells Penetrating Protective Coal Pillars in Longwall Mining Areas. *Processes* **2025**, *13*, 47. [CrossRef]
17. Zhang, H.K.; Guo, X.F.; Yang, K.L. Stress Zoning Characteristics of Goaf Side and Quantitative Evaluation of Surrounding Rock Stability. *Processes* **2024**, *12*, 2490. [CrossRef]
18. He, Y.; Zheng, Y.Z.; Xia, H.W.; Guo, F.L.; Yang, Q.F.; Wang, H. Study on risk assessment model for wellbore integrity. *Drill. Prod. Technol.* **2020**, *43*, 12–16+1.
19. Zhang, J.H.; Li, G.F.; Meng, Z.P.; Zhang, Y.C.; Liu, L.L.; Li, D.H.; Xu, Y. Key technology of surface extraction for coalbed methane wells crossing goaf. *J. China Coal Soc.* **2020**, *45*, 2552–2561. [CrossRef]
20. Li, J.J.; Li, G.F.; Hao, H.J.; Hao, C.S.; Wang, Z. Technology of across-goaf drainage of coalbed methane from a lower coal seam group and its primary application: Taking Sihe mine field as an example. *Coal Geol. Explor.* **2021**, *49*, 96–104.
21. Meng, Z.P.; Li, G.F.; Yang, Y.; Li, C.; Qiao, Y.D. Study on key technology for surface extraction of coalbed methane in coal mine goaf from Sihe Wells Area, Jincheng. *Coal Sci. Technol.* **2021**, *49*, 240–247. [CrossRef]
22. Liu, K.P.; Hu, S.Y.; Zhang, S.X.; Su, Y.; Zhang, Y.; Jin, T.X.; Zhang, C.; Hu, J. Research on key technology of L type coalbed methane well drilling through goaf. *China Energy Environ. Prot.* **2024**, *46*, 263–268+274. [CrossRef]

23. Li, C.X. Research and application of liner drilling tool in goaf of coal mine. *Coal Mine Mach.* **2021**, *42*, 137–140. [CrossRef]
24. Liu, X.G.; Zhang, Q.; Cui, W.H. Key drilling technology of L type gas extraction horizontal well through goaf. *Saf. Coal Mines* **2023**, *54*, 33–38. [CrossRef]
25. Lou, Y.; Liang, L.J.; Cheng, J.; Shao, L.J.; Yang, F.Q.; Yi, W. Research on directional drilling technology for superimposed "three zones" passing through goaf. *Coal Sci. Technol.* **2023**, *51*, 148–157. [CrossRef]
26. Pan, R.X.; Liu, J.M.; Cheng, H.; Fan, H.X. Study on the vertical stability of drilling wellbore under optimized constraints. *Appl. Sci.* **2024**, *14*, 2317. [CrossRef]
27. Zhang, H.; Xu, L.H.; Yang, M.M.; Deng, C.B.; Chen, Y.P. Pressure relief mechanism and gas extraction method during the mining of the steep and extra-thick coal seam: A case study in the Yaojie No. 3 coal mine. *Energies* **2022**, *15*, 3792. [CrossRef]
28. Gao, D.L. *Down-Hole Tubular Mechanics and Its Applications*; China University of Petroleum Press: Beijing, China, 2006.
29. Terzaghi, K.; Peck, R.B.; Mesri, G. *Soil Mechanics in Engineering Practice*; John Wiley & Sons: New York, NY, USA, 1967.

Disclaimer/Publisher's Note: The statements, opinions and data contained in all publications are solely those of the individual author(s) and contributor(s) and not of MDPI and/or the editor(s). MDPI and/or the editor(s) disclaim responsibility for any injury to people or property resulting from any ideas, methods, instructions or products referred to in the content.